

Communication

Not peer-reviewed version

# Designing Advanced Multistatic Imaging Systems with Optimal 2D Sparse Arrays

[Lorena Perez-Ejio](#)\*, [Marcos Arias](#), [Borja González-Valdés](#), [Yolanda Rodríguez-Vaqueiro](#),  
Oscar Rubiños-López, [Antonio Pino](#), Ignacio Sardinero-Meirás, Jesús Grajal

Posted Date: 28 September 2023

doi: 10.20944/preprints202309.2012.v1

Keywords: Submillimeter wavelength imaging; multistatic imaging; backpropagation imaging; genetic algorithm (GA).











Preprints.org is a free multidiscipline platform providing preprint service that is dedicated to making early versions of research outputs permanently available and citable. Preprints posted at Preprints.org appear in Web of Science, Crossref, Google Scholar, Scilit, Europe PMC.

Copyright: This is an open access article distributed under the Creative Commons Attribution License which permits unrestricted use, distribution, and reproduction in any medium, provided the original work is properly cited.

## Article

# Designing Advanced Multistatic Imaging Systems with Optimal 2D Sparse Arrays

Lorena Perez-Eijo<sup>1,\*</sup> , Marcos Arias<sup>1</sup> , Borja Gonzalez-Valdes<sup>1</sup> ,  
Yolanda Rodriguez-Vaqueiro<sup>1</sup> , Oscar Rubiños<sup>1</sup> , Antonio Pino<sup>1</sup> ,  
Ignacio Sardinero-Meirás<sup>2</sup>  and Jesús Grajal<sup>2</sup> 

<sup>1</sup> AtlanTTic Research Center, Universidade de Vigo, 36310 Vigo, Spain

<sup>2</sup> Information Processing and Telecommunications Center, Universidad Politecnica de Madrid, 28040 Madrid, Spain; [jesus@gmr.ssr.upm.es](mailto:jesus@gmr.ssr.upm.es)

\* Correspondence: [lorena@com.uvigo.es](mailto:lorena@com.uvigo.es)

**Abstract:** This study introduces an innovative optimization method to identify the optimal configuration of a sparse symmetric 2D array for applications in security, particularly multistatic imaging. Utilizing Genetic Algorithms (GA) in a sophisticated optimization process, the research focuses on achieving the most favorable antenna distribution while mitigating the common issue of secondary lobes in sparse arrays. The main objective is to determine the ideal configuration from specific design parameters, including hardware specifications such as number of radiating elements, minimum spacing, operating frequency range, and image separation distance. The study employs a cost function based on the the point spread function (PSF), the system response to a point source, with the goal of minimizing the secondary lobe levels and maximizing their separation from the main lobe. Advanced simulation algorithms based on Physical Optics (PO) are used to validate the presented methodology and results.

**Keywords:** Submillimeter wavelength imaging; multistatic imaging; backpropagation imaging; genetic algorithm (GA).

## 1. Introduction

Active millimeter and sub-millimeter-wave radar systems have become indispensable tools for enhancing civil security in airports, bus stations, crowded areas, and other public places [1]. These non-destructive testing (NDT) systems play a key role in security screening, imaging concealed objects and detecting weapons and drugs, providing effective and safe solutions. However, current monostatic or quasi-monostatic radar systems [2] face limitations in complex geometries due to shadow regions caused by specular reflections falling outside the receiving area.

To overcome this limitation, our proposal integrates multiple wideband millimeter-wave transmitters and receivers to obtain high-resolution radar images in real time [3,4]. Multistatic systems offer several advantages, such as improved detection of stealth objects, reduced susceptibility to interference, and the ability to acquire information from multiple angles. This approach also allows the use of a lower spatial sampling frequency than conventional systems by taking advantage of the cancellation of the secondary lobes.

This paper presents a novel methodology for identifying the optimal 2D sparse matrix configuration to generate multi-static images based on predefined design parameters. Section 2 introduces the architecture, the imaging procedure, and the function that will be used to evaluate possible solutions. In Section 3, we provide an introduction to GAs and explain their specific application to this work. The simulation process is defined in Section 4, while Section 5 presents the obtained results, including a compelling comparison between optimized and non-optimized approaches. Finally, in Section 6 we summarize the achieved objectives and outline potential future approaches to further enhance the efficiency of imaging systems.

## 2. Multistatic architecture

The architecture of the system relies on multiple transmitters ( $tx_m$ ) and receivers ( $rx_n$ ), positioned at  $t_m$  and  $r_n$ , respectively [5,6]. Typically, these systems employ large, densely sampled arrays (Eq. 1) to ensure sufficient Fourier space (k-space) coverage, which aids in achieving high resolution by minimizing the presence of secondary lobes.

$$d_{elements} \leq \frac{\lambda_{min}}{2} \quad (1)$$

The main purpose of these systems is to be used in real-time personnel security and surveillance applications. Hence, it is crucial to minimize the number of required elements.

### 2.1. Baseline configuration

This work serves as a prelude to the production of a prototype, which is already in the construction phase. As a result, design constraints have been defined by considering the available hardware and its specific characteristics. Our focus is on analyzing a specific architecture consisting of a 2-D sparse array with 64 transmit antennas (NTX) and 49 receive antennas (NRX) positioned in front of an Object Under Test (OUT). The transmit antennas are spaced equidistantly at a distance of  $d_{tx}$  cm, while the receive antennas are also equidistantly spaced at a distance of  $d_{rx}$  cm. To ensure symmetrical responses with respect to both the  $X=0$  and  $Z=0$  axes, this equidistance is maintained in both the horizontal and vertical directions. The system operates in the frequency range of 120 to 150 GHz using only 12 different frequencies, which corresponds to a minimum working wavelength ( $\lambda_{min}$ ) of 2 mm.

### 2.2. Imaging

The imaging process implies generating an image for each transmitting antenna, with each image being formed by coherently summing the contributions from individual receptors. The final image is obtained by coherently combining these transmitter images. Figure 1 provides a graphical representation of the described procedure on a simplified system with  $NTX = 3$  and  $NRX = 2$ .

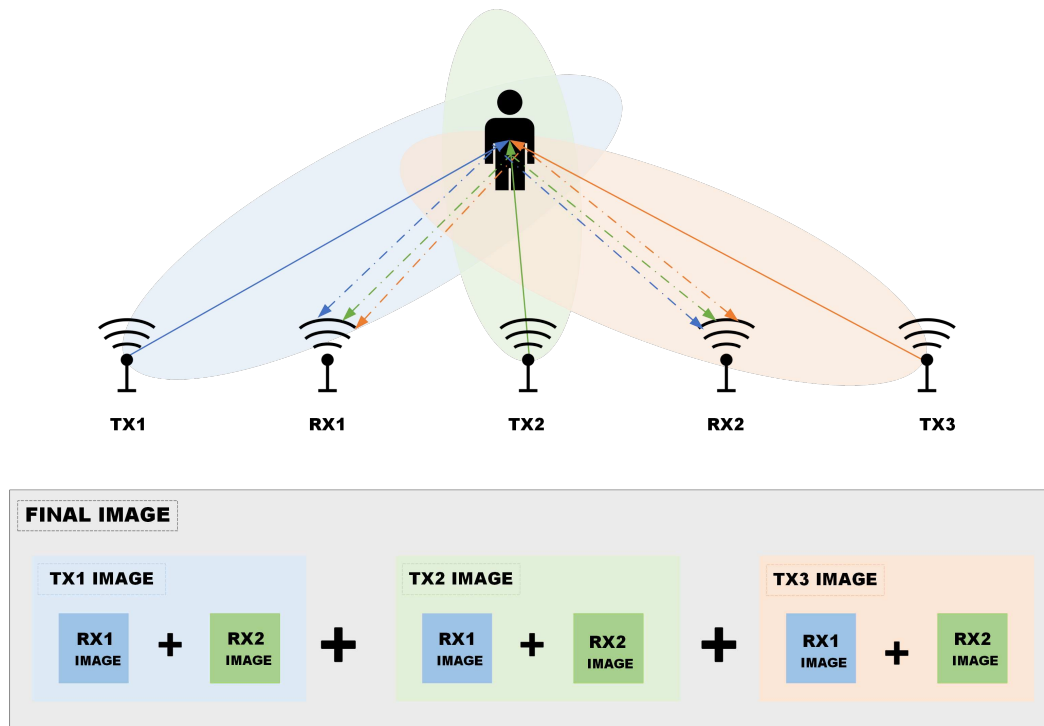


Figure 1. Graph of the imaging process in a simplified system with  $NTX = 3$  and  $NRX = 2$ .

### 2.3. Point spread function

One of the most useful parameters to characterize the behavior of an imaging system is the PSF, which describes the response of a system to a point source target. Based on the reciprocity theorem, the total PSF of the system when focused at the point  $\mathbf{p}_i$  can be calculated from the PSFs of the transmit and receive arrays as follows [4]:

$$PSF_{rx}(\mathbf{p}_i) = \sum_{l,n} e^{-j\kappa_l |\mathbf{r}_n - \mathbf{p}_i|} \quad (2)$$

$$PSF_{tx}(\mathbf{p}_i) = \sum_{l,m} e^{-j\kappa_l |\mathbf{t}_m - \mathbf{p}_i|} \quad (3)$$

$$PSF_{total}(\mathbf{p}_i) = PSF_{rx}(\mathbf{p}_i) \times PSF_{tx}(\mathbf{p}_i) \quad (4)$$

where multiple frequencies  $f_l$  are used to generate the images in an Ultra Wide Band (UWB) radar configuration, and  $\kappa_l$  is the wavenumber at the  $l$ -th frequency. The PSF calculation is employed to determine the optimal array size for the imaging system.

Knowledge of the PSF is invaluable in many ways. It plays a key role in determining the resolution of the system, which represents the size of the main beam, and also provides valuable information about the dimensions and position of the secondary lobes surrounding the main beam. The presence of secondary lobes is a critical factor because it directly affects the quality of the images produced by the imaging system. To achieve the desired results, it is important to identify a configuration with a minimum number of secondary lobes. It has been observed that it is also beneficial to place these secondary lobes as far away from the main lobe as possible. This helps reduce aliasing between responses and increases the field of view (FoV) of the system, improving its imaging capabilities.

### 3. Genetic Algorithm

GAs have proven to be effective in finding solutions to real-world problems [7,8]. They operate on a population of individuals, where each individual represents a potential solution to the problem at hand. The fitness of each individual is evaluated based on its ability to solve the problem. Highly fit individuals are given the opportunity to reproduce by mating with other individuals in the population, resulting in an offspring that inherits certain characteristics from their parents. Through this process, less fit individuals are less likely to be selected for reproduction and eventually die out, leading to the emergence of a new population with potentially better solutions. The algorithm combines the best individuals from the current generation with recombination (crossover) and mutation to create a new set of individuals. As a result, successive generations tend to improve upon the previous ones as the best-performing individuals reproduce and exchange genetic information. By encouraging the combination of the most promising individuals and using mutations to avoid optimization stalling, genetic algorithms are able to efficiently explore the most favorable regions of the search space. The basic operation of GA is depicted in Figure 2.

A well-designed GA is capable of converging on an optimal solution to a given problem. A notable strength of GAs is their ability to handle diverse problem domains, including those that are traditionally challenging for other methods. Since GAs cannot guarantee to find the globally optimal solution due to their inherent randomness, there is a possibility that they will converge to a local minimum without reaching the optimum. Nevertheless, GAs are generally capable of quickly finding solutions that are good enough for practical purposes.

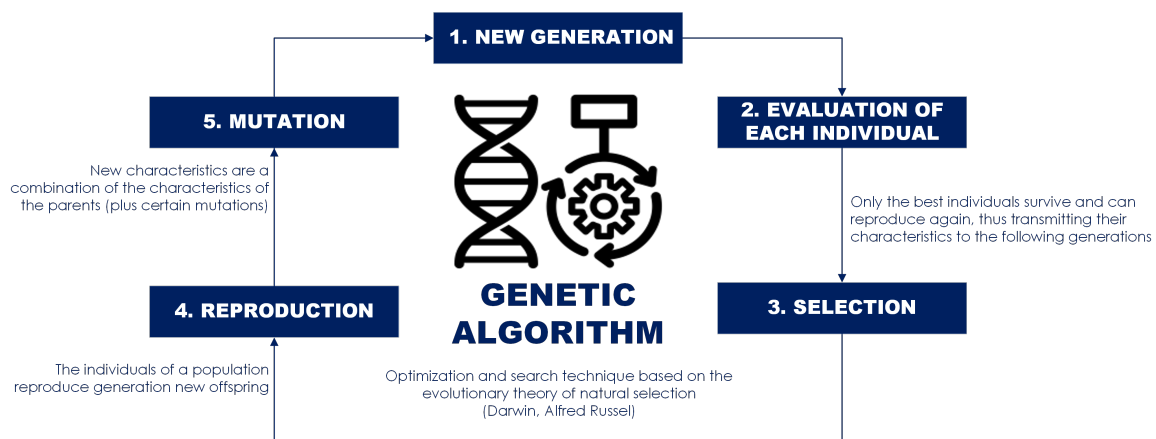


Figure 2. Basic GA operation.

### 3.1. Custom GA configuration

In this work, GA is used to compute the optimal value of the distance between the receiving elements ( $d_{rx}$ ) while keeping the distance between the transmitting elements ( $d_{tx}$ ) fixed. When we first started using GAs, attempts were made to optimize both variables simultaneously, but it turned out that setting the value of  $d_{tx}$  to cover the desired aperture and calculating the optimal value of  $d_{rx}$  proved to be more efficient.

To evaluate which values are most appropriate, a custom cost function is defined based on the PSF of the system. The best configuration will be the one with the lowest sidelobes. As stated in Section 2.1, this work corresponds to the pre-prototype phase, so the configurations must satisfy specific design constraints:

- The aperture size (horizontal and vertical) cannot exceed 100 cm.
- Due to hardware limitations, the minimum distance between elements is set to 2 cm.
- The array is symmetric on both the X and Z axes.
- Transmitter elements are equispaced in two dimensions (both horizontally and vertically). So are the receivers.

The process is computationally expensive as the GA solver needs to construct the corresponding architecture, calculate the PSF, and evaluate the cost function for each possible pair of  $d_{tx}$ - $d_{rx}$  values. Despite this, utilizing GPU acceleration and MATLAB's vector computation capabilities allows us to obtain preliminary results quickly and efficiently. Fixing  $d_{tx}$  and optimizing only for  $d_{rx}$  yields results in less than 3 minutes and 18 seconds. If  $d_{tx}$  and  $d_{rx}$  are optimized simultaneously, the process takes approximately 15 minutes.

## 4. Simulation

A PO based simulator for THz imaging systems is used [9,10]. The simulator performs a two-step simulation of the electromagnetic response of the imaging system to an arbitrary OUT. In the first step, the simulator calculates the induced electric currents in the OUT by considering the interaction between the incident electromagnetic wave and the material properties and geometry of the OUT. By solving Maxwell's equations, the simulator determines the distribution of the induced currents on the surface of the OUT. The simulator then calculates the field received at each receiver from the field generated by the eddy currents. This process is repeated independently for each transmit antenna and each single frequency ( $f_l$ ).

For radiation modeling, both the transmit and receive antennas are represented as ideal spherical sources. The OUTs are imported into the simulator as CAD models. Reflectivity images are obtained by applying SAR techniques, as referenced in [11]. The final reflectivity image is normalized to its maximum value for display purposes.

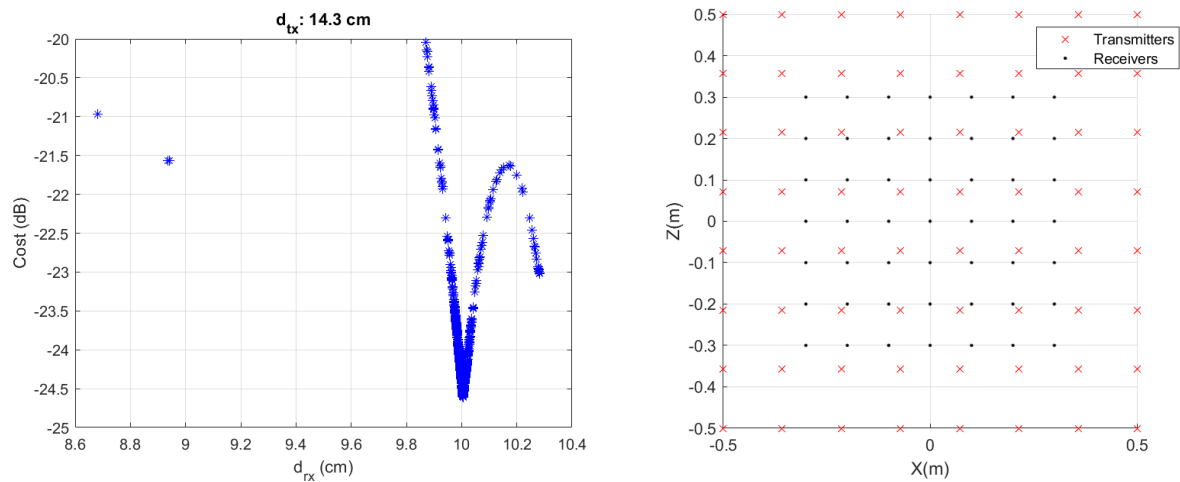
## 5. Results

The results presented were obtained using the hardware described below:

- HW-1: Laptop
  - 12th Gen Intel® Core™ i7-12700H @ 2.70 GHz
    - \* RAM: 32 GB
    - \* Number of Cores: 14 (20 logical cores per physical)
  - 1 × NVIDIA GeForce RTX 3070 Ti Laptop GPU
    - \* Memory: 8 GB (GDDR6 SDRAM)
    - \* Number of CUDA Cores: 5888
- HW-2: Server GPU
  - 32 × 13th Gen Intel® Core™ i9-13900K @ 5.80 GHz
    - \* RAM: 128 GB
    - \* Number of Cores: 24 (32 logical cores per physical)
  - 1 × NVIDIA GeForce RTX 4090
    - \* Memory: 24 GB (GDDR6X)
    - \* Number of CUDA Cores: 16384

### 5.1. Optimal 2D-sparse array

To prove the performance of the method, an architecture with 64 transmitter elements (NTX) and 49 receiver elements (NRX) is used. The desired aperture size is 1 m, both in range and cross-range. To achieve the desired aperture size,  $d_{tx}$  is set to 14.3081 cm. Considering the physical characteristics of the array elements, a minimum spacing of 2 cm is maintained between them. As previously mentioned, the system operates in the frequency range of 120 GHz to 150 GHz. Considering all these design factors, the initial step involves using GA to determine the optimal  $d_{rx}$ . Figure 3 (a) shows the values taken by  $d_{rx}$  in a given optimization and the associated costs until the optimal value is reached. The optimization results yielded  $d_{rx} = 10.0103$  cm, which is utilized to construct the optimal architecture (Figure 3 (b)).



(a) Values taken by  $d_{rx}$  during optimization and associated costs. GA convergence at 10.0103 cm

(b) Optimized architecture

**Figure 3.** Optimal 2D-sparse array architecture via GA ( $\frac{d_{rx}}{d_{tx}} = 0.7$ ).

#### 5.1.1. PSF

Figure 4 displays the PSF at 3 meters of the architecture that was constructed from the value obtained in the GA optimization. The presence of the secondary lobes is observed about  $\approx 13$  cm from



the main lobe and with a magnitude 24.6 dB below that of the main lobe. Figure 4 shows the PSF in (a) XZ plane and (b) X cut when  $Z = 0$ .

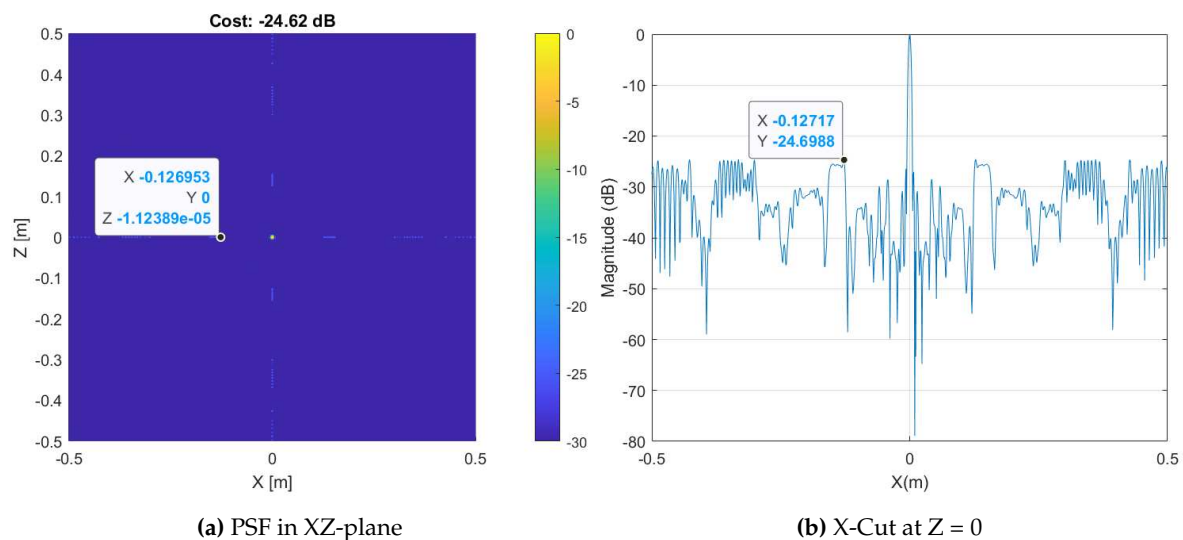


**Figure 4.** PSF of optimal architecture at a standoff distance of 3 m.

The nature of these architectures and the non-compliance with the Nyquist criterion make the presence of these diffraction lobes inevitable, which limits the FoV of the reconstruction and directly affects the quality of the images that the system can produce.

Without the aid of these tools, the most intuitive way to design the architecture would be to distribute the transmitters and receivers equidistantly along the X and Z axes. Thus, to achieve an aperture of 1 m, the distance between the elements should be 13.33 cm. Figure 5 (a) shows the resulting configuration and Figure 5 (b) shows the PSF response at 3m. The presence of several secondary lobes extremely close in magnitude to the main lobe is not a good sign, as it implies a significant degradation in the quality of the recovered images. The improvement of the optimized system over the non-optimized one is remarkable.

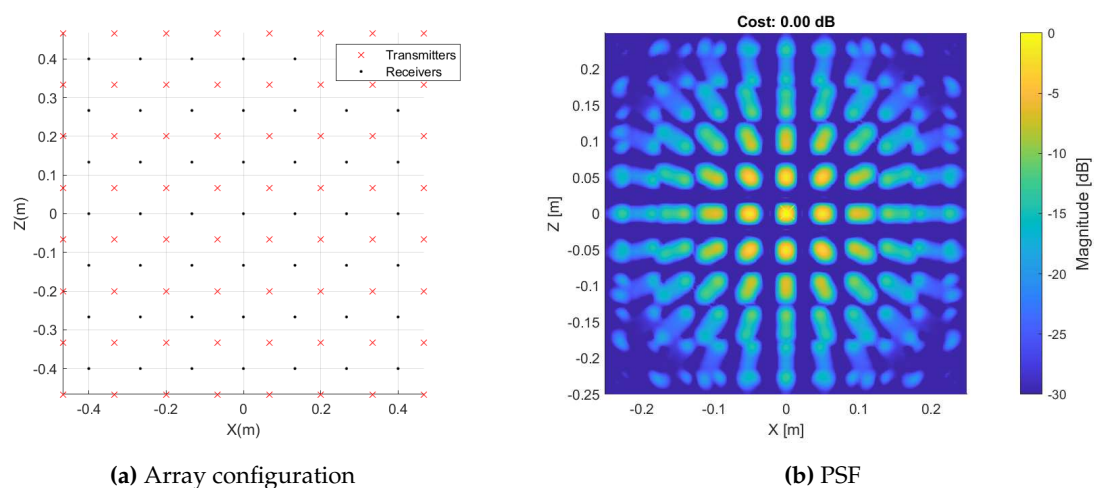


**Figure 5.** Non-optimized array configuration and its corresponding PSF.

### 5.1.2. Imaging

To validate the performance of the presented configuration, a model based on a 1951 USAF MIL-STD-150A resolution test chart was used as OUT. This type of geometry consists of several groups of bars (in this specific case modeled as metal plates) separated by a certain distance, and is widely used to analyze and validate imaging systems. The CAD model used in the following simulation is

shown in Figure 6 (a) and Table 1 specifies its geometry.

To perform the experiment, the OUT is placed at a standoff-distance of 3 m. As can be seen in Figure 6 (b), the reconstruction replicates all the details of the original image. This shows that the system has a very high resolution, since it is able to reconstruct all the elements of the two groups of bars, which indicates that it is able to detect targets with an accuracy of less than 1 mm.

**Table 1.** Custom 1951 USAF MIL-STD-150A model geometry definition.

RESOLUTION (rr) ANALYSIS		
DISTANCE BETWEEN BARS		
GROUP NUMBER		
ELEMENT	-2	-1
1	2.5 cm	0.85 cm
2	1.75 cm	0.75 cm
3	1.5 cm	0.5 cm
4	1 cm	0.25 cm
5		0.2 cm
6		0.1 cm
Vertical spacing between elements		
1 cm		
Bar width (bw)		
1 cm		
Bar length (bl)		
$3bw + 2rr$		

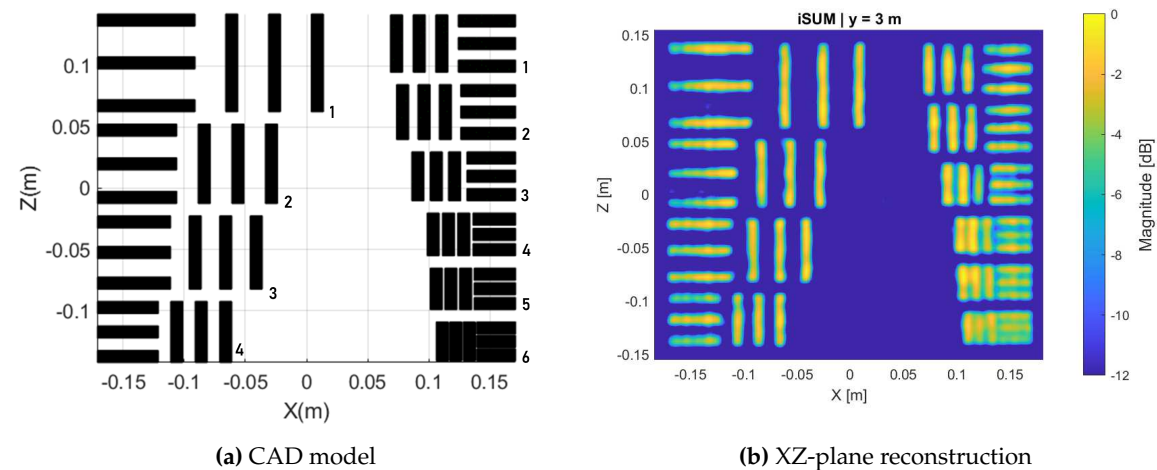


**Figure 6.** XZ-plane reconstruction of the USAF-based target located 3 m from the antenna array.

**Runtime simulation performance**

To perform the imaging, an XZ plane of 36.5 cm × 31 cm is defined. A 2.5 mm discretization is used, so the image plane consists of 18375 pixels. As explained in Section 2.2, each  $tx_m$ - $rx_n$  pair generates an individual image, leading to a total of 3.136 different images to combine for this architecture. HW-1 processes images in 0.03 seconds, but with HW-2, it achieves an impressive 0.008 seconds – a remarkable improvement. This exceptional performance is attributed to the utilization of GPU resources and MATLAB’s vector computing capabilities.

Our commitment to achieving greater efficiency and faster processing speeds motivates us to constantly enhance the software. We strive to explore alternative approaches that optimize performance and push the boundaries of what is currently achievable.

**6. Conclusions**

This study introduces a method for designing 2D-sparse arrays, resulting in remarkable improvements in imaging performance. By integrating advanced electromagnetic simulation and



powerful mathematical optimization algorithms (GA), this approach yields highly satisfactory results. It demonstrates the capability to achieve superior reconstruction outcomes while utilizing less than 2% of the elements typically required by conventional full-density 2D arrays.

The significance of this method extends to the development of On-The-Move (OTM) imaging systems, enabling real-time 3D imaging of moving targets. The reduction in the number of elements, combined with optimized simulation codes utilizing vector computation in Matlab and harnessing the potential of GPU and parallelization resources, drastically minimizes the execution time of the simulations.

This study represents a remarkable advancement in imaging technology, offering promising possibilities for more efficient and agile imaging systems with unparalleled imaging quality. This research makes a significant contribution to the field of image processing and paves the way for future advances in the field.

**Acknowledgments:** This work was supported by projects PID2020-113979RB-C21 and PID2020-113979RB-C22 funded by MCIN/AEI/10.13039/501100011033 and by the European Union NextGenerationEU/PRTR under project RYC2021-033593-I.

**Conflicts of Interest:** The authors declare no conflict of interest.

## References

1. Ahmed, S.S. Personnel screening with advanced multistatic imaging technology. SPIE Defense, Security, and Sensing. International Society for Optics and Photonics, 2013, pp. 87150B–87150B.
2. Grajal, J.; Badolato, A.; Rubio-Cidre, G.; Úbeda Medina, L.; Mencia-Oliva, B.; Garcia-Pino, A.; Gonzalez-Valdes, B.; Rubiños, O. 3-D High-Resolution Imaging Radar at 300 GHz With Enhanced FoV. *IEEE Trans. Microw. Theory Tech.* **2015**, *63*, 1097–1107. doi:10.1109/TMTT.2015.2391105.
3. Gonzalez-Valdes, B.; Rappaport, C.; Martinez Lorenzo, J.A. On-the-move active millimeter wave interrogation system using a hallway of multiple transmitters and receivers. 2014 IEEE Antennas and Propagation Society International Symposium (APSURSI), 2014, pp. 1107–1108. doi:10.1109/APS.2014.6904880.
4. Gonzalez-Valdes, B.; Rodriguez-Vaqueiro, Y.; Alvarez, Y.; Heras, F.L.; Garcia, A.P. Nearfield-based array design for a realistic on-the-move personnel inspection system. 2017 11th European Conference on Antennas and Propagation (EUCAP), 2017, pp. 2846–2850. doi:10.23919/EuCAP.2017.7928214.
5. Gonzalez-Valdes, B.; Alvarez, Y.; Mantzavinos, S.; Rappaport, C.M.; Las-Heras, F.; Martinez-Lorenzo, J.A. Improving Security Screening: A Comparison of Multistatic Radar Configurations for Human Body Imaging. *IEEE Antennas and Propagation Magazine* **2016**, *58*, 35–47. doi:10.1109/MAP.2016.2569447.
6. Gonzalez-Valdes, B.; Vázquez-Cabo, J.; Rodriguez-Vaqueiro, Y.; Álvarez, Y.; Garcia-Fernandez, M.; Arboleya, A. Array Optimization for an On-The-Move 3D Imaging System Demonstrator. 2018 IEEE International Symposium on Antennas and Propagation USNC/URSI National Radio Science Meeting, 2018, pp. 1961–1962. doi:10.1109/APUSNCURSINRSM.2018.8608606.
7. Holland, J.H. *Adaptation in Natural and Artificial Systems*; University of Michigan Press, 1975. second edition, 1992.
8. Beasley, D.; Bull, D.R.; Martin, R.R. An Overview of Genetic Algorithms: Part 1, Fundamentals. *University Computing* **1993**, *15*, 58–69.
9. Arias-Acuña, M.; Garcia-Pino, A.; J.O. Rubiños-Lopez. Fast far field computation of single and dual reflector antennas. *Journal of Engineering* **2013**, *2013*, 11. doi:10.1155/2013/140254.
10. Perez-Eijo, L.; Gonzalez-Valdes, B.; Arias, M.; Tilves, D.; Rodriguez-Vaqueiro, Y.; Rubiños-López, O.; Pino, A.; García-Rial, F.; Grajal, J. A Physical Optics Simulator for Multireflector THz Imaging Systems. *IEEE Transactions on Terahertz Science and Technology* **2019**, *9*, 476–483. doi:10.1109/TTHZ.2019.2930918.
11. Wehner, D.R. *High-resolution Radar*, second ed.; Artech House, 1995.

**Disclaimer/Publisher's Note:** The statements, opinions and data contained in all publications are solely those of the individual author(s) and contributor(s) and not of MDPI and/or the editor(s). MDPI and/or the editor(s) disclaim responsibility for any injury to people or property resulting from any ideas, methods, instructions or products referred to in the content.